RSC Advances

A systematic understanding of gelation self-assembly: Solvophobically assisted supramolecular gelation *via* conformational reorientation across amide functionality on a hydrophobically modulated dipeptide based ambidextrous gelator, N-*n*-acyl-(L)Val-X(OBn), (X = 1,ω-amino acid)

Saubhik Haldar* and Koninika Karmakar

Department of Chemistry, Jadavpur University, Kolkata, West Bengal, INDIA

*Corresponding author
Email: shaldar@chemistry.jdvu.ac.in ; saubhikhaldar@gmail.com
Phone no: +91 33 2414 6223, Fax. No. +91 33 2414 6223

ABSTRACT

A systematic investigation on gelation self-assembly has been performed on a hydrophobically modulated dipeptide based ambidextrous gelator, N-n-acyl-(L)Val-X(OBn), (X = 1,ω-amino acid). To elucidate the effect of hydrophobic tuning on gelator architecture towards its gelation self-assembly, three sets of gelators with a common formula: $C_mH_{2m+1}C(=O)NH(L)Val(C=O)NH-(CH_2)_n-(C=O)OBn$, were synthesized , Set- I includes gelators with n = 2, m = 9,11,13,15,17, for Set-II it is n = 2,3,5, m=13 and Set-III comprises of two isomeric gelators (n=2, m=15; n=10, m=7). Gelation has been critically analyzed in various apolar (aromatic and aliphatic) and polar (protic and aprotic) solvents using FESEM, CD, IR, WAXRD and rheological studies. Obtained results reveal that π-π type interaction dictates the primary molecular alignment and positioning of amide functionality across the aliphatic chain which influences the peptidic orientation in parallel (when m > n) or antiparallel (when m < n) β-sheet type organization in their self-assembly. The thermal stability, gelation number (GN), T_{gel} and yield stress of gel systems increases with m, but for a given m, the trend goes apparently inverse with increasing n. Circular dichroism (CD) studies suggest an intriguing evidence of non-planarity of amide plane during self-assembly, highlighting the involvement of conformational change taking place during molecular organization towards its gelation. Despite complex nature of solvent-gelator interaction, the effect of H-bonding component of solubility parameters was found to have a significant role on self-assembly. Overall, supramolecular forces acting at specific functionalities encrypted in gelator backbone must overcome the solvation energy with synergic assistance of solvophobic effect towards stabilization of gel-network with optimum gelator backbone conformation for achieving required enthalpic contribution for self-assembly.

1. Introduction

Despite ample information being available on various gel forming molecular backbones, designing of a gelator molecule using existing models capable of gelating in a particular liquid have limited scope as the fundamental understanding of the particularities and characteristics of molecular self-assembly resulting in gelation is still inadequate.[1] A rapid growth in the research area of supramolecular low molecular weight organo-gelator (LMOG) has been witnessed due to their diverse application in miscellaneous fields.[2-7] Constant efforts have been directed to understand the rationale behind the formation of such soft materials arising from spontaneous self-assembly of low molecular weight scaffolds[8] and more specific to biocompatible peptide based systems.[9] Inherent chirality of amino acids with a variety of side chain residues can impart a remarkable influence on non-covalent molecular association with interactive amide linkages on their supramolecular properties that give rise to anisotropic aggregation towards amyloid-like fibrillar structures[10] and a subsequent non-covalent cross linking of these fibrils leads to the formation of fibrous network that restricts flow of the entrapped solvent, resulting in gelation. The major challenge in designing a new gelator requires adequate understanding of relative contributions of various intermolecular interactions among the gelator molecules,[11] gelator–solvent[12] and the mechanism involved[13] in their gelation process. Efforts have been made by various research groups toward this direction.[14-17] Utilizing the van der Waals interaction in long hydrophobic aliphatic chains with a short peptide H-bonding sequence, gelation has been observed in polar solvents.[18-19] A rational approach of mastering the competing dynamic interaction and hierarchical phase organization of non-covalently bound organic moieties in the dynamic self-assembly was employed by Barboiu et. al.[20] Introduction of functional groups into an already studied gelator skeleton could be another strategy of getting functional organogels.[21] However, such approach has a possible inconvenience towards aggregation properties being significantly altered due to new functionalization which can compete with H-bonding or alter solubility profile.[22] Another systematic

investigation was performed by Fages and co-workers with a library of N-acyl-1,ω-amino acid derived gelators wherein the gelation ability was remarkably influenced by the type of aromatic substituted N-acyl pendant, amino acid chain and also the degree of ionization of the carboxylate group.[23] A structure-function relationship with the mesophases of the gels obtained from amino acid derived dimeric dendrons was correlated with different aliphatic spacers on the gelator backbone.[24] However Suzuki et. al. showed that gelation of N-alkyl amino acid amide of valine and isoleucine with 1,ω-dicarboxylic acid and its monoester depends very much on the nature of their terminal functionality.[25] Choice of amino acid as chiral spacer on the gelator backbone was addressed recently by Bhattacharya et. al[26] and our group.[27] Amino acid derived biologically inspired gelators can self-assemble via H-bonding even in polar solvents due to large number of donor sites available per molecule and the gelation efficiency improves as the number of peptide unit increases.[28] The past, present and future direction of molecular gel have been nicely described in a recent review by Richard G. Weiss where it has been clearly mentioned that a very limited scope still prevails in designing molecular gelators based on various models, rather the major dominance exists in the serendipitous discoveries of new structural classes of gelators.[29] Earlier, we have shown that peptide sequence or even the peptide architecture can modulate the self-assembly property in a remarkable fashion.[30] In the present study, a systematic variation at the hydrophobic substituents on the molecular backbone of gelator has been made and a rationalization towards structure function relationship has been attempted elucidating the controlling factors behind their gelation self-assembly. A series of low molecular weight (L)Val based dipeptidic ambidextrous gelators, N-n-acyl-(L)Val-X(OBn), (X = 1,ω-amino acid)[more specifically, $C_mH_{2m+1}C(=O)NH(L)Val(C=O)NH-(CH_2)_n-(C=O)OBn$], were synthesized: Set- I (n = 2, m = 9,11,13,15,17), Set-II (n = 2,3,5, m=13) and Set-III comprises of two isomeric gelators (n=2, m=15; n=10, m=7)(shown in Fig. 1) and their gelation behavior was carefully studied using established experimental protocols. The experimental results were carefully analyzed to find out the rationale of structural modulation over their gelation such self-assembly.

[Fig.1]

2.   Materials and Methods

2.1.   Materials

Dicyclohexylcarbodiimide (DCC), L-valine and all other 1,ω-amino acids (β-alanine, γ-aminobutyric acid, 6-aminocaproic acid, 11-aminoundecanoic acid) were purchased from Sigma chemicals. Long chain fatty acids, 1-hydroxybenzotriazole (HOBT) were purchased from SRL, INDIA, and N-hydroxysuccinimide (NHS), K_2CO_3 were purchased from Spectrochem, India. Solvents were purchased from SD fine chemicals, India and were freshly distilled before use. Silica gel G has been used for TLC and iodine vapor as staining agent.

2.2.   Synthesis

The L-Val based dipeptidic gelators (**4a**- **4h**) have been synthesized in our laboratory following the given scheme of synthesis. The details of the synthetic procedures, ^{1}H and ^{13}C NMR, and mass spectroscopic data have been provided in the supporting information.

2.3.   Determination of Critical Gelation Concentration (CGC) and Gelation number (GN)

The gelators were insoluble in almost all solvents used in this study at room temperature; however, they get dissolved on heating, which gelates on cooling. The critical gelation concentration (CGC) as well as gelation number (GN) has been determined by dissolving known amount of gelator in specific volume of a solvent, gelating them in identical vials bringing them at room temperature and taking into account of the solvents gelated by the specific gelators.

2.4.   Determination of Gel Melting Temperature

Gel to sol transition temperature (T_{gel}) of the gels was determined using vial inversion method[31] as well as by oscillatory temperature-sweep rheology as has been described by Menger et. al.[32] In the former method, the T_{gel} has been defined as the temperature at which the gel melts and begins to flow out of the vial. Where as in case of later method, the T_{gel} has been taken as the temperature at which

Scheme of synthesis
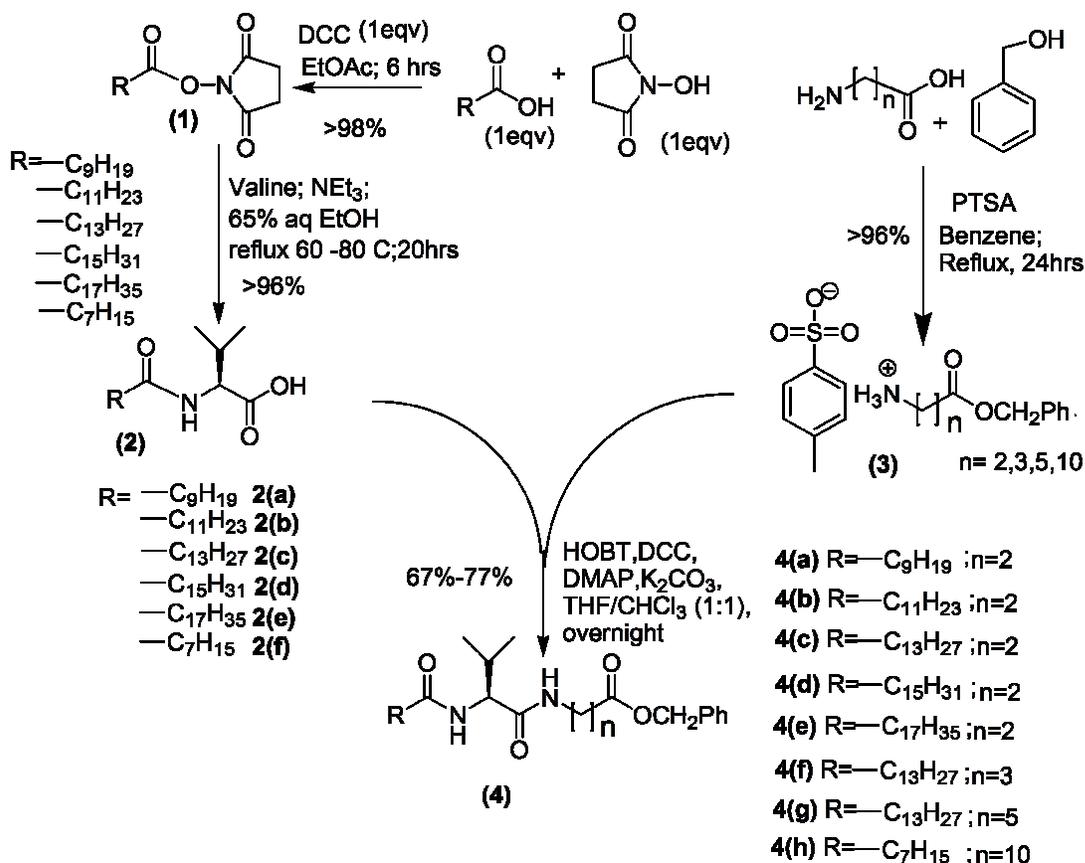
the elastic modulus (G') drops below the viscous modulus (G") indicating the point at which gel breaks under applied stress. The gel–sol transition temperatures (T_{gel}) of the organogels were determined for various solvents at different concentrations using the vial-inversion method. The vials containing the gels were placed upside down on a water bath fixed with a high-precision temperature regulator and heated. The bath was warmed up at the rate of about 0.1°C per sec. The temperature, at which the gel started to flow, was taken as T_{gel} of the organogels.

2.5.   FTIR Spectroscopy.

Spectra were collected using a BRUKER ALPHA FT-IR spectrometer with ATR attachment for the

gelators in solution (in $CHCl_3$) as well as in their gel state (in acetonitrile).

2.6.   WAXRD study of thin film of xerogel

Organogels prepared in different solvents (acetonitrile, ethanol, 80% (v/v) ethanol in water,

anisole, etc.) were spread on glass cover slips and air dried carefully. The obtained films of these air

dried gels (xerogels) were subjected to WAXRD studies using Bruker D8 Advance with a parallel beam

optics attachment. The instrument was operated at a 35 kV voltage and 30 mA current using Ni-filtered

CuK_α radiation and was calibrated with a standard silicon sample. Samples were scanned from 0° to 30°

in the step scan mode (step size 0.020, preset time 2 s) and the diffraction patterns were recorded using

a scintillation scan detector.

2.7.   Circular Dichroism

CD spectra were recorded using a Jasco (model J-815) CD spectrometer with a band width of 1

nm and slit width of 100 µm in the ultraviolet region (190-350 nm) and a quartz cuvette of 1 mm path

length. Experiments were performed with a sample interval of 0.5 nm and scan speed of 200 nm/min at

a controlled temperature of 20 °C. The samples for the experiment were prepared at different

concentrations.

2.8.   Field emission scanning electron microscopy

Morphologies of the gel materials were investigated using FESEM instrument INSPECT F50 (The

Netherlands) with an acceleration voltage of 20 kV. For this study, samples of the xerogels were

prepared on a glass slide and scratched carefully and placed on carbon tape and coated with a thin layer of gold.

2.9.   Rheology

Rheological Frequency sweep experiment was performed at 25 °C using an MCR-102 rheometer (Anton Paar) with a cone plate (40 mm diameter and cone angle 1 degree) at a gap setting of d = 0.080 mm, linear frequency range of 1.0 to 10.0 Hz and constant strain of 0.01%. Rheological oscillatory strain sweep experiment was also executed with the same instrument at a strain amplitude (γ) ranging from 0.01 % to 100% and a constant angular frequency of 10 rad s^{-1}.

3.   Results and Discussion

3.1.   Designing of Gelator molecules

A schematic representation of the gelators with modified segments is shown in Fig. 2. The design comprises of four functionally distinct regions, viz, (i) an aromatic unit (benzyl ester) placed at one end of the molecular backbone,(ii) a dipeptidic unit arising from peptide bonds between (L)-Valine and 1,ω-amino acid residues, (iii) a flexible hydrophobic spacer sandwiched between aromatic and peptidic zone and (iv) n-acyl chain with different molecular length connected to the N-terminal of the dipeptide. These give rise to three sets of gelators having a common formula of $C_mH_{2m+1}C(=O)NH(L)Val(C=O)NH-(CH_2)_n-(C=O)OBn$ with varied m and n values. The gelator architecture comprised of these four segments exhibiting specific supramolecular interactions based on their inherent functionalities. A π-π type interaction is presumably evident at segment (i), whereas H-bonding interaction is expected from segment (ii), and van der Waals type interaction likely to be predominant at segments (iii) and (iv).

[Fig.2]

In this paper, effect of hydrophobic modulation at the backbone architecture on the gelation self-assembly has been rationalized by systematic variation at the segment (iii) and (iv) keeping invariable units at segment (i) and (ii) which gives rise to three sets of gelators. Set-I gelators (**4a**- **4e**) consisting of varied N-*n*-acyl chain lengths (m = 9,11,13,15,17) with a given spacer (n = 2), ostensibly addresses the effect of systematic increment in hydrophobicity at the N-acyl region on their gelation behavior. Fine tuning of hydrophobicity at the spacer region [segment (iii)] (with n = 2, 3, 5) has been focused in Set-II gelators, **4c**, **4f** and **4g** where n values are 2, 3 and 5 for a given n-acyl chain (m = 13) respectively. The reason behind choosing m = 13 is due to the fact that it is the average acyl chain length among the all acyl units. Interestingly, Set-III includes two isomeric gelators of identical molecular length **4d** (n=2, m=15) and **4h** (n=10, m=7) with peptidic zone placed at different positions addressing the issues of how the mutual placement of amide functionality at different depths in the gelator backbone affects the gelation. Another possible isomer with n = 15 and m=2 was excluded for the present study on the basis of the fact that the amide unit in this isomer would be placed almost at the other termini of the gelator backbone and this will lead the gelator to possess two functionalities (π-π interactive unit and amide unit) having directional non-covalent interactions at the two ends and it needs to be dealt separately.

3.2. Morphology

Vial inversion method was employed to sight the gelation and field emission scanning electron microscopy (FESEM) to examine the self-assembled 3D network in gel matrix. The formation of organized nanostructures, such as nanofibers, nanoribbons, and nanosheets has been widely found in supramolecularly interactive organogels.[33-34] We have taken three representative gelators **4d**, **4g** and **4h** from Set-I, II and III respectively (Fig. 3) and studied their molecular network in acetonitrile. In either of the cases, fibrillar network (a prerequisite for a gel like system) with a rod like architecture was observed in higher resolution and the dimensions of the nanofibers look different in each of these cases. As the

respective xerogels were obtained in the identical solvent, the variation in nano-structuring is seemingly due to differences in molecular architecture.

[Fig.3]

3.3.   Gelation behavior

The gelators have been showing an ambidextrous type gelation behavior with very high gelation ability in various apolar and polar solvents (both protic and aprotic) including aqueous alcoholic media (detailed data given in in S.I Table S1). The gels were stable for weeks and do not transform into viscoelastic fluids or crystallize on prolonged storage in stoppered vessel at room temperature in closed vials. The critical gelation concentration (CGC) has been expressed in terms of gelation number (GN)[35] which is defined as the number of solvent molecules that is entrapped in the gel matrix per gelator molecule. The change in hydrophobicity of the gelator molecules due to structural modulation has been compared based on their clogP values. The clogP is calculated logP where P is defined as the ratio of the equilibrium concentration of a substance dissolved in a two-phase system formed by two immiscible solvents, octanol and water. The effect of hydrophobic modulation on gelator backbone architecture on their GN in various solvents has been depicted in Fig. 4 where, Panel-I describes GN vs. clogP for Set-I gelators in solvents like, (a) aromatic, (b) apolar, (c) polar aprotic and (d) polar protic media and Panel-II depicts the same for Set-II gelators. In general, GN increases with the increase in N-acyl chain length attached to the amide unit but not in a linear fashion where **4d** (with C(16:0) N-acyl chain) shows exceptionally high GN values than any other system. Comparatively lower GN for **4e** (with C(18:0) acyl chain) indicates that longer acyl chain might not always help in having higher gelation number. A very interesting observation has been encountered in case of Panel-I(b) representing the change in GN with respect to clogP in apolar solvent like cyclohexane and *n*-hexane for Set-I gelators; a reverse trend, i.e., GN decreases with the increase in clogP, was observed in *n*-hexane but an usual increasing trend was found in cyclohexane. Seemingly, the gelation self-assembly gets more and more unfavorable with the

increase in N-acyl chain length in *n*-hexane than it occurs in cyclohexane. Owing to an extended and flexible conformation compared to rigid cyclic structure of cyclohexane, *n*-hexane can preferably interact with the N-acyl motif with higher van der Waals interaction and thus N-acyl chains get solubilized more in *n*-hexane than in cyclohexane giving rise to lower GN with higher clogP. Although, for Set-I gelators, the GN value increases with the increase in acyl chain length, such increasing trend is neither linear nor of an equal extent in different media. This suggests that, increase in intergelator van der Waals stability cannot be the sole reason behind better gelation self-assembly. An analogous understanding was cited by Iqbal et. al. where, solvophobic interactions are expected to be important for aliphatic chains in polar solvents, however it may not be contributing significantly to the 1D-aggregation for long and flexible chains.[36] While comparing the effect of increase in hydrophobicity at the spacer region for Set-II gelators, GN reduces with the increase in clogP via increase in methylene units in the spacer region (as the n-acyl chain was kept identical for all cases here). A drastic decrease in GN takes place with increase in spacer length from $(CH_2)_2$ (**4c**) to $(CH_2)_3$ (**4f**) but it increases again in $(CH_2)_5$ (**4g**), i.e., the trend is like **4c>4g>4f**. This could be due to the fact that instability in molecular packing takes place while going from $(CH_2)_2$ (**4c**) to $(CH_2)_3$ (**4f**) resulting in decrease in GN values; however a solvophobic interaction might start occurring in case of **4g**, as it can also be observed that GN value of **4g** in aprotic polar solvent is comparatively more than in apolar and aromatic solvents (Fig. 4 Panel-II). Considering the hydrophobicity and conformational flexibility exerted by aliphatic tail and the spacer region, apparently a critical balance between mutual placement of π-π interactive aromatic units and H-bonding zone of amide play an important role in augmenting the stability of the self-assembly in a synergic fashion. This is demonstrated by evaluating the gelation ability of Set-III gelators, where in one of the isomeric gelators **4h** for which H-bonding zone is deeply seated with respect to π-π interactive motif. Thus it loses its gelation ability even in hydrophobic media (e.g. pet-ether, hexane etc.) but shows gelation in aromatic solvents. The enthalpic contribution from amide unit alone is insufficient

11

to stabilize the self-assembled network because the aliphatic zone (N-acyl / spacer) offers more gelator-solvent interaction in apolar solvents rather in aromatic ones. On the other hand a polarophobic collapse helps in self-assembly for **4h** in aprotic polar solvents. Moreover, the destruction of intergelator H-bonding network in polar protic solvent hinders the formation of self-assembly of **4h** where the polarophobic interaction might be insufficient for the self-assembly. Thus a polarophobic interaction must be synergistically assisted by H-bonding interaction along with suitably placed other supramolecular units with optimum flexibility to exhibit stable self-assembly. As has been highlighted by van Esch et. al. that the direct relation of gelation strength with the changes in solvent properties is not possible and it is more complex in nature, like, the hydrogen bonding interactions were weaker in polar solvents whereas the gelation occurred only where sufficient compensation was provided by intergelator van der Waals interactions.[37]

[Fig.4]

3.4.   Thermal stability of Gels

Gel to sol transition temperature (T_{gel}) of the gels was determined by vial inversion method as well as by temperature-sweep oscillation rheology and T_{gel} values obtained from either of the methods were found concurrent with each other (see SI, Figure. S5-S7).In general, the thermal stability increases with the increase in the N-acyl chain length as the result obtained from T_{gel} vs. clogP plot for Set-I (Fig.5 Panel-I). But in the case of **4d**, T_{gel} was found to be considerably very high in aprotic polar solvents like, DMSO, acetonitrile, acetone and moderately higher in aromatic solvents like toluene, anisole and xylene whereas it falls within the expected range in EtOH or in MeOH. Therefore, clogP alone cannot describe the thermal stability of the gels for Set-I. In case of Set-II (Fig. 5. Panel-II), T_{gel} however decreases in general with the increase in clogP though not linearly (**4c**>**4g**>**4f**). Thus, the increase in aliphatic spacer might increase the hydrophobicity (clogP) but decreases the thermal stability eventually. Interestingly, **4d** and **4h** (showing gelation in few solvents) of Set-III having comparable clogP values (structural

isomers) **4h** with a very high spacer length has much lower T_{gel} compared to **4d** (see SI), presumably

higher conformational flexibility at spacer region affecting the molecular packing in case of **4h**.

Therefore, hydrophobic interaction at the N-acyl chain or at the spacer region cannot solely govern the

gelation process. While correlating the gelation number (GN) with the T_{gel}, it was observed that data

remains invariant or scattered signifying T_{gel} is not strictly dependent on GN values (SI, Figure Table 1). In

other words, higher GN might not reflect in their better molecular packing. This was also corroborated

with the rheological studies.

[Fig.5]

Concentration dependence on T_{gel} values show (Fig. 6) that the T_{gel} increase with the concentration of

gelators and from this, the thermodynamic parameters ($\Delta H°$, $\Delta S°$ and $\Delta G°$) at 298 K of gels (from

different gelators) in acetonitrile were calculated (Table 1) following the reported procedures.[38-39] The

results show that the values of $\Delta G°$ were in agreement with the trend of T_{gel} of the gelators in CH_3CN.

Moreover, T_{gel} of the gelators were compared at two distinct concentrations: 0.166 mM and 0.244 mM

as the former concentration is before reaching the plateau region and the later one after achieving the

plateau of T_{gel} vs [Gelator] plot (Fig. 6). The difference in the trend in T_{gel} values indicates that

reorganization in the gelation self-assembly takes place with the increase in concentration.

[Fig.6]

Table1 Calculated thermodynamic parameters of the gelators in acetonitrile at 298 K

GELATORS	$\Delta H°$(kJ/moles)	$\Delta S°$(J/moles)	$\Delta G°$(kJ/moles)
4a	91.78	278	8.83
4b	83.68	243	11.27
4c	147.35	445	14.74
4d	108.51	310	15.62
4e	99.02	286	13.80
4f	98.07	295	10.16
4g	50.85	137	9.87
4h	43.72	123	7.07

3.5.   Rheology.

A quantitative estimation of viscoelastic properties of the materials was performed by oscillatory rheological experiments. From an experimental point of view a gel is composed of two component (solvent and gelator) viscoelastic system that exhibits two distinct mechanical properties: (i) the system should not flow under a mechanical stress lesser than a limiting value, called yield stress and (ii) it must be more elastic than viscous.[40] The viscoelastic response of the material is characterized by two material measures, i.e, the elastic storage modulus G' and the viscous loss modulus G'' and measured by dynamic oscillatory rheological strain sweep experiments.[41] This study gives an indication of the flow behavior and rigidity of the gel. The storage modulus (G') [the ability of the deformed material to store energy] and the loss modulus (G'') [the flow behavior of the material under stress] are the two main parameters for the evaluations of the mechanical strengths of the gel system. In the gel state, $G'>G''$ and in the sol state, $G''>G'$. The crossover point between G' and G'' indicates the transition point from elastic solid to viscous liquid, whereas yield stress is defined as the minimum stress that must be applied to a sample in order to induce flow. This is determined by strain sweep experiments and the stress value at which G'' becomes higher than G' is measured for **4a-4h**. Fig.7 depicts a representative

plot of strain-sweep experiment (G', G'' vs. Strain) for **4a**, **4c, 4g** and **4h**. In case of Set-I gelators, yield stress were found to be 189 (**4a**), 205 (**4b**), 262 (**4c**), 392 (**4d**) and 260 (**4e**); for Set-II : 262 (**4c**); 215 (**4f**); 98 (**4g**), and for Set-III : 392 (**4d**); 625 (**4h**). The results seemingly demonstrate that the yield stress increases with the increase in the acyl chain length; however it shows an opposite trend with the increase in spacer length. Such results corroborate with the results obtained for the T_{gel} values. However, in case of Set-III, for isomeric gelators, **4h** shows an unusual behavior where the yield stress is higher in comparison to **4d** but T_{gel} of **4h** is less than **4d**. Shear elasticity, yield stress and melting behaviors were correlated to the cross-sectional sizes of fibers gel networks by Terech et. al.[42]where the lowering of melting point attributing to the regions of solid and liquid are large enough so that contributions from their surfaces is negligible, however the higher yield stress can be ascribed to the internal strength of the aggregated structure and results from the balance of structural breakdown and recovery of rheologically active units. To discern the discrepancy for **4h**, it can be endorsed that, polarophobic interaction might help to increase entanglement of fibrous network leading to higher junction points and contribution from surfaces increases, however self-assemblies with higher conformational flexibility at the backbone architecture led to its lower melting point. The presence and extent of elasticity in a fluid gel systems were also analyzed using their tan δ values which represents the ratio of viscous modulus (G'') to elastic modulus (G'). The tan δ value of less than unity indicates elastic-dominant (i.e. solid-like) behavior and values greater than unity indicate viscous-dominant (i.e. liquid-like) behavior. In Set-I [0.210 (**4a**), 0.220 (**4b**), 0.190 (**4c**), 0.104 (**4d**), 0.235 (**4e**)], tan δ values were found to decrease with the increase in acyl chain length; however tan δ values are comparable among gelators in case of Set-II [0.190 (**4c**), 0.149 (**4f**), 0.199 (**4g**)] and Set-III [0.104 (**4d**), 0.100 (**4h**)], though Set-II has comparatively higher values than Set-III. Therefore, Set-I elasticity increases with the increase in acyl chain length which corroborates with yield stress and T_{gel} data. However it was not significantly different in case of Set-II. Interestingly, a comparable elasticity was observed for Set-III gelators. Based on the

obtained tan δ values ranging from 0.10–0.22 in the frequency sweep measurements, the systems can

be considered as strong gels where the storage modulus G' is on average about 6–9 times greater than

the loss modulus G".[43] The increase in the elastic modulus of an organogel, as perceived by Rogers et.

al., is due to an increase in fibre–fibre interactions which lead to the formation of greater number of

transient junction zones, in turn leading to a more ordered system. [44]

[Fig.7]

3.6. FT-IR Studies

To investigate the inter-gelator interaction at the peptidic region and the ester functionality near the

aromatic substituent, FT-IR studies were performed to identify the changes on the vibrational spectra of

the non-covalently interactive functional units in gel and sol state of the gelators. Since amide-I and

amide-II bands are two most prominent vibrational bands to identify protein secondary structures,[45] we

tried to analyze the H-bonding network exist in the present series of gelation self-assembly. The

accompanied band shift of non H-bonded amide in soluble state to the H-bonded amide in the gel state,

the difference in vibrational mode at two states was tried to be identified by FT- IR. Analysis of the FT-IR

spectra of gelators 4a - 4h has been performed in solution ($CHCl_3$) as well as in gel state in acetonitrile

(shown in Table 2). The amide I vibration, (absorbing near 1640 cm^{-1}) arises primarily from the C-O

stretching vibration along with a minor contributions from the out-of-phase C-N stretching vibration,

the C-C-N deformation and the in plane bending of NH. In the present case, all the systems show

absorption within the range of 1630-1643 cm^{-1} which lie within the characteristic amide-I   band for

parallel β-sheet type amide network. Moreover, amide-II band within the range of 1540-1547 cm^{-1} also

support the parallel β-sheet type arrangement. Usually, the amide II band arises from the out-of-phase

combination of the NH in plane bend and the CN stretching vibration with smaller contributions from

the CO in plane bend and the C-C and N-C stretching vibrations. While comparing the data for **4d** and **4h**,

a striking difference was observed. A parallel β-sheet type arrangement was evident all the gelators

having shorter spacer unit (m > n) but with larger spacer unit (m < n, **4h**) additional absorption bands at

1697 cm^{-1} and 1507 cm^{-1} (along with 1632 and 1546 cm^{-1}) was observed suggesting a mixed β-sheet

type peptidic network (parallel and antiparallel). The shifting of amide-A band at higher wave number

while going from solution phase to gel phase also indicates the participation of N-H unit in H-bonding

interaction. Primarily an invariant band at ~1735 cm^{-1} , assigned for ester C=O, across all the gelators at

their gel or sol state suggests its nonparticipation in H-bonding.[44] Keeping the results in proper

perspective, two types of molecular organizations have been postulated which is depicted in the Fig. 8.

Because of the molecular structures, π-π interaction among aromatic units makes the molecule to stay

in such a way that for gelators with shorter spacer (m > n, **4a** -**4g**) interdigitation might occur at the N-

acyl unit keeping the amide units in a parallel fashion in either orientation: along the plane and at its

orthogonal direction (between the layers). But for longer spacer (n > m, **4h**) interdigitation occurs with

an antiparallel β-sheet type interaction among the amide units where the N-acyl units stabilized by van

der Waals interaction with the spacer region and a parallel β-sheet type interactions may occur between

such planes at orthogonal direction. Such molecular arrangement might suggest to have a lower d$_{100}$

value for **4h** which is experimentally supported by XRD data where the d$_{100}$ for **4h** is found to be shorter

than **4d**. (see XRD discussion).

<div align="center">[Fig.8]</div>

3.7. Wide Angle X-Ray Diffraction

The packing pattern in the supramolecular assembly was analyzed using wide-angle X-ray

diffraction (WAXRD) spectra of the xerogels **4a** - **4h** in acetonitrile and also, **4c** and **4g** in a set of

different solvent systems to find out the solvent effect on molecular packing with respect to structures

bearing different spacer length. The obtained results were found to be in good agreement with the

proposed parallel β –sheet arrangement with π-π type interactive aromatic moieties in the

supramolecular network. A low-angle sharp peak with respect to (1 0 0) plane was attributed to the

depth of the self-assembly present in the molecular network and it lies between 20 to 26 Å which is close to the extended length of a single gelator molecule. Considering the π-π type interactive aromatic units forming an extended network keeping the molecule in one particular orientation with parallel beta sheet type H-bonded peptidic zone, the (1 0 0) reflection might be coming from the next π-electron rich aromatic layer in opposite direction with an interdigitated network architecture (Fig. 10). Such organization is also evident in literature.[47] The data corresponding to d_{100} spacing (firstorderreflection),interlayerspacing,π-πstackingandedgelengthofcubiclattice(a) have been presented in Table 3. In case of XRD pattern of Set-I gelators in acetonitrile, the d-spacing increases with the increase in chain length, however, gelators with very long hydrophobic chain, was found to have a considerable low value in d-spacing, suggesting a self-assembly having interdigitation with higher tilt angle. Peaks assigned to a periodic distance of 3.89 Å were found ascribing to extended two-dimensional layers of β -sheets that stack parallel on top of each other.[34] While analyzing the diffraction pattern using the plot of 1/d vs. $(h^2 +k^2 + l^2)^{\frac{1}{2}}$ a straight line passing through the origin suggests the gelation self- assembly presumably possesses a primitive cubical phase (*Pm3m*) with a comparable lattice parameter (a), however intensities of some of the reflections were too low to detect. A representative plot for **4d** in acetonitrile and **4g** in acetonitrile and ethanol is presented in Fig. 9 (for details, see SI Figure S9-S17). The major diffraction patterns (in hkl) as obtained in acetonitrile media from the gels have been presented below.

Set I: XRD patterns of the following gelators in acetonitrile.

4a: (1 0 0), (2 0 0), (2 1 0), (2 2 0), (3 2 2).

4b: (1 0 0), (2 0 0), (2 2 0), (4 3 2).

4c: (1 0 0), (1 1 0), (1 1 1), (2 2 0), (2 2 2), (4 0 0), (4 3 2).

4d: (1 1 0), (2 0 0), (2 1 1), (4 0 0), (4 2 2).

4e: (1 0 0), (1 1 0), (1 1 1), (2 2 0).

Set II: XRD patterns of the following gelators in acetonitrile.

4c: (1 0 0), (1 1 0), (1 1 1), (2 2 0), (2 2 2), (4 0 0), (4 3 2).

4g: (1 0 0), (2 0 0), (2 1 0), (2 2 0), (2 2 2), (4 2 0), (5 4 2).

Set II: XRD patterns of the following gelators in Anisole.

4c: (1 0 0), (1 1 0), (1 1 1), (2 0 0), (2 1 0), (2 2 0), (2 2 2), (4 2 0), (4 2 2).

4g: (1 0 0), (1 1 0), (1 1 1), (2 0 0), (2 1 0), (2 2 0), (3 3 2).

Set II: XRD patterns of the following gelators in EtOH.

4c: (1 0 0), (1 1 0), (1 1 1), (2 2 0), (3 2 0), (3 2 2), (3 3 2).

4g: (1 0 0), (1 1 0), (2 0 0), (2 1 1), (3 0 0), (3 2 0), (3 3 2), (4 2 2), (4 3 1).

Set II: XRD patterns of the following gelators in 80% (v/v) EtOH in water.

4c: (1 0 0), (1 1 0), (1 1 1), (2 1 0), (2 2 2), (3 3 1), (4 2 2).

4g: (1 0 0), (1 1 0), (2 0 0), (2 1 0), (2 2 2), (3 3 2), (3 3 3), (4 3 2).

Set III: XRD patterns of the following gelators in acetonitrile.

4d: (1 1 0), (2 0 0), (2 1 1), (4 0 0), (4 2 2).

4h: (1 0 0), (1 1 0), (1 1 1), (2 0 0), (3 2 0), (4 2 0).

[Fig.9]

To find out the effect of solvents on the molecular packing of self-assembly, we have taken two

different gelators **4c** and **4g**. Since 4c being a representative of both Set-I and Set-II can give insights for

both the series. Similarly, comparison between **4c** and **4g** (for Set-III gelators) can give the effect of

solvents on the molecular packing for Set-II gelators. The XRD patterns as observed for both the gelators

in four different media has been presented below.

4c in

Acetonitrile: (1 0 0), (1 1 0), (1 1 1), (2 2 0), (2 2 2), (4 0 0), (4 3 2).,

Anisole: (1 0 0), (1 1 0), (1 1 1), (2 0 0), (2 1 0), (2 2 0), (2 2 2), (4 2 0), (4 2 2).

EtOH: (1 0 0), (1 1 0), (1 1 1), (2 2 0), (3 2 0), (3 2 2), (3 3 2).

80% (v/v) EtOH in water: (1 0 0), (1 1 0), (1 1 1), (2 1 0), (2 2 2), (3 3 1), (4 2 2).

4g in

Acetonitrile: (1 0 0), (1 1 0), (2 0 0), (2 1 0), (2 2 0), (2 2 2), (4 2 0), (5 4 2).

Anisole: (1 0 0), (1 1 0), (1 1 1), (2 0 0), (2 1 0), (2 2 0), (3 3 2).

EtOH: (1 0 0), (1 1 0), (2 0 0), (2 1 1), (3 0 0), (3 2 0), (3 3 2), (4 2 2), (4 3 1).

80% (v/v) EtOH in water: (1 0 0), (1 1 0), (2 0 0), (2 1 0), (2 2 2), (3 3 2), (3 3 3), (4 3 2)

The obtained results suggest that, the d-spacing is affected while going from aromatic to aliphatic

solvents as well as, going from protic polar (EtOH and 80 % (v/v) EtOH in water) to aprotic polar

(Acetonitrile). Incorporation of more H-bonding acceptor in the solvent matrix, e.g. 80% (v/v) EtOH in

water compared to EtOH, the d spacing reduces going from aprotic to protic. But the over-all packing

does not show much alteration from primitive cubical arrangement. Such cubic gels are found to have

wide applications in pharmaceutical sciences as an efficient drug delivery system.[48] More details of the

solvent effect will be discussed later but it is quite evident that an increase in polarity makes the gelator

more compact in their molecular packing. Thus, the molecular structure certainly plays a dominant role

in determining the molecular organization in the gelation self-assembly. A similar observation was also

encountered by Iqbal et. al.[34] where they observed that for a given compound, there were not

important differences in the position of the diffraction peaks between different solvents: attributing to

the fact that although macroscopic properties such as solubility or gelation efficiency are strongly

solvent dependent, the solvent has a limited effect in the organization at the molecular level. Using

molecular mechanics (using CS Chem3D ultra version 7.0) the molecular length of **4d** has been

calculated and a gelator self-assembly was made for molecular mechanics energy minimization which

suggests considerable interdigitation among the acyl chains with calculated d_{100} values to be ~46.4 Å,

however d_{100} obtained by XRD measurements is 21 Å, suggesting that the interdigitated self-assembly

might have a tilt angle of ~60°. The lower d_{100} value of 17.0 Å for **4h** compared to 21.05 Å for isomeric

gelator **4d** suggest a compact molecular packing in the self-assembly for the former one. In our view,

corroborating with the IR results, an interdigitated antiparallel organization of the gelator (**4h**) might

take place in the β-sheet arrangement as shown in Fig. 10(c) with a similar tilt angle as that of the

others.

[Fig. 10]

3.8. Circular dichroism

Initial formation of one dimensional supramolecular network via self-assembly of gelator

molecules was found to be an important event for the generation of 3D entangled fibrils in gelation

process. To discern such event for the present set of gelators, a concentration dependent circular

dichroism experiment was performed. To avoid the scattering effect, we had to carry out the

Table 3 d_{100} spacing corresponds to first order reflection, interlayer spacing, π-π stacking and edge length of cubic lattice (a).

gelators	d_{100} (in Å)	a (in Å)	Interlayer spacing (in Å)	π-π stacking distance (in Å)
4a in CH$_3$CN	21.01	21.07		3.86
4b in CH$_3$CN	22.57	22.20	5.88	3.87
4c in CH$_3$CN	19.18	19.83	5.63	3.81
4c in EtOH	20.62	20.55	5.65	3.82
4c in 80%aq EtOH	19.74	20.63	5.68	3.80
4c in anisole	20.52	22.37	5.68	3.84
4d in CH$_3$CN	21.05	21.04	5.68	3.89
4e in CH$_3$CN	21.43	20.20	5.67	3.90
4g in CH$_3$CN	22.06	22.66	5.68	3.84
4g in EtOH	22.00	22.24	5.66	3.83
4g in 80%aq EtOH	19.18	19.83	5.63	3.81
4g in anisole	21.01	20.33		3.87
4h in CH$_3$CN	17.00	18.36	5.69	3.76

experiment at a concentration much lower than their corresponding CGC values to keep them at the

soluble state. In general, all the gelators showed very much similar strong positive couplet in CD spectra with a higher wavelength (n→π*) negative cotton band at ~238 nm and a positive cotton band at lower wavelength region (π→π*). A considerable red shift was found in the CD spectra for n→π* band with the increase in concentration of the gelator. This could be due to the deviation of the planarity of amide functionality in the self-assembly at higher concentration. Such observation was nicely described by Lucie et. al. in their computational studies on the spectroscopic properties of nonplanar amide groups.[49] Therefore, such phenomena suggest a significant conformational change on the gelator backbone is associated with the formation of gel network at higher concentration. Unequal amount of red-shift of CD band at higher wavelength for different gelators also suggest that, nevertheless the amino acid is identical in all cases, the conformational flexibility of the hydrophobic segments at the spacer and/or the acyl chain does influence differently on the gelator self-assembly.[50]

[Fig.11]

3.9. Solvent effect

Solvent effect on gelation behavior at its macroscopic level has been discussed by various research groups using different solubility parameters of the solvents related to their nonspecific and specific intermolecular forces.[51] Hanabusa and co-workers reported that the minimum gelation concentration of cyclo-(dipeptides) in various organic solvents could be correlated with a polar solubility parameter (δ_a) of the solvents.[50] The general relationship between macroscopic gelation and solvatochromic parameters based on a multi-parameter approach to solvent polarity using Kamlet-Taft parameters were reported by Smith and co-workers.[53-54] However, a linear correlation between T_{gel} values and the dielectric constants of alcoholic solvents were reported by Makarevic and co-workers for the gelation of different bis (amino acid) oxalyl amides.[55] Intermolecular forces are usually classified into two distinct categories. The first category comprises the so-called directional, induction, and dispersion forces, which are non-specific and cannot be completely saturated whereas the other category consists

of specific and directional forces like, hydrogen-bonding forces, charge-transfer or electron-pair donor – acceptor forces which can be saturated and lead to stoichiometric molecular compounds. We discuss the gelation ability of the gelators **4a**-**4h** with respect to three different solubility parameters of solvents,[56] viz, (a) Dimroth-Reichardt $E_T(30)$ parameter, (b) Hansen-Beerbower solubility parameters (HSP) and (c) Kamlet-Taft parameters. $E_T(30)$ parameter signifies the ionizing power (loosely polarity) of the solvents. However, HSP comprises of three components which involves (i) energy from dispersion bonds between the molecules (δ_d), (ii) energy from dipolar intermolecular forces (δ_p) and (iii) energy from hydrogen bonds between molecules (δ_h). The δ_o and δ_a are the total solubility parameter and the polar solubility parameter respectively. The total solubility parameter δ_o has been described as $\delta_o^2 = \delta_d^2 + \delta_a^2$ where $\delta_a^2 = \delta_p^2 + \delta_h^2$. For small molecules, ($\delta_o$) is equated to the cohesive energy that is required to overcome the intermolecular forces. Parameters of the Kamlet–Taft solvatochromic relationship which measure the hydrogen bond donor (α), hydrogen bond acceptor (β), and dipolarity/polarizability (π^*) properties of solvents as contributing to overall solvent polarity. These usually relate to the overall solvation ability for the solutes at the ground state and/their excited state. Although no direct correlation between GN and $E_T(30)$ was observed, a moderate decrease in GN was observed in aromatic solvents with the increase in $E_T(30)$ values. However, a reasonable increase in GN with $E_T(30)$ was observed in polar protic / aprotic solvent systems. Due to a wide distribution of gelating solvents in 3D HSP space, no significant region of solvents was found to be apparent to predict the gelation behavior. In order to have a mutual dependence of any two of these parameters on gelation behavior, plots of, δ_p vs δ_h, δ_d vs δ_h and δ_p vs δ_d were examined and presented in Fig. 12 Panel-I, which suggests more clustering of data in the encircled area indicating δ_h has preferentially more impact on the gelation behavior than δ_p or δ_d since in the plots without δ_h shows no clustering of gelating solvents was observed in comparison to other two cases. Interestingly, this observation is applicable for all the gelators, **4a**- **4h,** however, the gelating solvents for **4h** apparently possess lower δ_h values. We also analyze HSP

parameters in terms of Tea's plot [see SI for details, Figure S24, S25] which also corroborates the former

observation. Finally, we tried to analyze the solvent effect using Kamlet-Taft solubility parameters (KT).

In this case as well, due to inability in identifying specific zone of gelation in 3D plots of KT parameters,

we plotted separately, π^* vs. α, β vs. α and β vs. π^* [Fig. 12, Panel-II] and found that H-bonding donating

ability of the solvent (i.e., α) significantly influences the gelation at its two regions, $0.0 - 0.2$ and another

between $0.8 -1.0$, however data was found to be more dispersed in case of β vs. π^* plot signifying its

lesser effect on the gelation behavior. Moreover, **4h** shows a single region of gelation in π^* vs. α and β

vs. α plot with lower α value as similar to the observation in case of HSP. Comparing, the isomeric

gelators in Set-III, **4d** and **4h**, the increase in spacer length reduces its gelation behavior in solvents with

higher α values signifying that H-bonding network gets destabilized in case of **4h** with the increase in

propensity of H-bonding donor ability of the solvents. Interestingly, **4h** loses its gelation ability in hexane

or cyclohexane while **4d** shows the ability to gelate. Again **4h** does not give any gelation in EtOH, MeOH

or isopropanol but gives gelation in acetonitrile, EtOAc and DMSO while **4d** is capable of giving gelation

in either of the solvents. The increase in spacer length helps the solvation in solvents with higher

dispersive interaction (as depicted by δ_d in HSP) however a polarophobic interaction with lower H-

bonding donating solvents helps in gelation for **4h**. On the contrary, **4d** with shorter spacer length is not

only capable of forming strong H-bonding network even in protic and aprotic solvents with high δ_p and

δ_h and with a broad range of α values in KT but also in hexane or in cyclohexane with very high δ_d and

very low δ_p and δ_h (in HSP) [See SI Figure S21] suggesting a synergic influence of polarophobic effect with

H-bonding interaction behind gelation behavior. Such gelation behavior is very much analogous to the

observation by Zweep et. al. in their cyclohexane based bisamide and bisurea organogelators where

they found that the H-bonding interaction were weaker in polar solvents and gelation occurred only

where sufficient compensation was provided by intergelator van der Waals interactions.[33] Solvophobic

interactions towards peptide based organogelation was also addressed by Loo et. al. describingtwo

types of interactions stabilize the self-assembled structures—solvophobic interactions with the solvent

molecules and interactions between solvophobic groups in the interior of the aggregate.[57]

[Fig.12]

3.10.Plausible mechanism behind the gelation self-assembly

Nevertheless, the nucleation and growth of gelation self-assembly is a complex stochastic

phenomena involving highly specific interactions that allow preferential one-dimensional growth driven

by enthalpic forces,[40] both gelator backbone architecture and the nature of the solvent-solute

interactions have been found to be crucial behind such process.[1, 14-17] Between the two extremes of

solute-solvent interaction of being soluble or insoluble, gelation self-assembly involves colloidal state

where the molecular organization is stabilized more by enthalpic contribution.[58]

[Fig.13]

A plausible rationale behind the mechanism of the present gelation self-assembly has been depicted in

Fig.13. Herein, the gelator backbone, for **4a**- **4h**, consists of four non-covalently interactive regions : A, B,

C and D; of which A, C region with aliphatic segment offering van der Waals interaction, whereas B

region is preferably interactive via H-bonding and π-π type supramolecular interaction is prevalent at

the region D. In a gelation self-assembly, solvent contributes itself as a major component of the matrix

where the gelator contributes ~2-3 wt% of the total mass. Being a colloidal suspension (neither a

solution nor a precipitate), solvent-solute interaction plays a major role towards self-assembly as well as

imparting strength and thermal stability to the gel matrix. The influence of gelator architecture and the

nature of gelating solvents have been correlated recently with the molecular packing within the one-

dimensional objects and the nature of the derived gels obtained from 12-hydroxystearic acid and its

isomers by Mallia et.al.[59]Between the two extremes of very high gelator-gelator and gelator-solvent

interactions would lead the gelator either insoluble or totally soluble respectively. Thus a critical balance

between gelator-gelator and gelator solvent interactions is a prerequisite for gelation behavior. Herein, the self-assembly has been analyzed in solvents of different nature, viz, aromatic, nonpolar, polar protic and polar aprotic with respect to their interactions towards A, B, C and D regions of **4a**-**4h**. At the monomeric stage, gelators are expected to be surrounded by the solvent molecules which interact non-covalently with the gelator back bone. Such solvent-gelator interaction is found to be very much decisive towards the formation of self-assembly of the gelators. In case of aromatic solvents, being quite apolar in nature, apolar part of the molecule (i.e., A, C and D), have favorable/stabilizing interaction (showing by ↓) with the solvent. Wherein aromatic zone (D) is expected to have preferentially more favorable π-π type solvent-gelator interaction in all the gelators of Set-I, II and III keeping the region B less interactive with the solvent. Therefore, in this case, the intergelator interaction leading to self-assembly is majorly dominated by intergelator H-bonding interaction. A very similar incident is also prevalent in case of non-aromatic apolar solvents except in case of **4h** of Set-III, where the longer spacer at C interacts with the hydrophobic solvent to such a high extent that merely H-bonding interaction cannot hold the self-assembly and no gelation takes place. In case of polar protic solvents, the polarophobic interaction [i.e., unfavorable gelator-solvent interaction (shown by↑)] of the hydrophobic parts (A, C and D) helps towards gelation self-assembly nevertheless H-bonding unit at B is capable of interacting with protic solvents. Such interaction is clearly demonstrated in Set-III systems, **4d** and **4h**. In protic polar solvents , a dominant polarophobic effect leads to gelation of **4d** similar to Set-I and Set-II, but **4h** fails to show gelation in similar media. Now the question arises, why doesnot the polarophobic effect itself helps in gelation of **4h** in polar protic solvents? A plausible reason being polarophobic interaction must be synergistically supported by H-bonding network. The thermotropic and rheological data indicates that the conformational flexibility at the spacer region reduces the gelation process, or in other words, the H-bonding network at amide zone (B) is augmented by the presence of aromatic unit at a critical distance but falls apart with an increase in spacer hydrophobicity (of aliphatic methylene units)

with more conformational flexibility. In case of polar aprotic solvents, polarophobic interaction plays a major role for self-assembly at the region A,C and D and such solvents are not expected to interact at the region B. Thus intermolecular H-bonding interaction is not destabilized by such solvent systems. Thus corroborating to the obtained results , the plausible mechanism can significantly emphasizes on the critical solvophobic/solvophilic balance across the gelator backbone architecture becomes a prerequisite for self-assembly where supramolecular functionalities encrypted on the backbone plays an important measure across intergelator interactions, however a solvophobic effect dominates in the gelationprocess towards achieving required enthalpic contribution for self-assembly.

4. CONCLUSION

Exploiting a systematic tuning of hydrophobicity at two distinct regions along a simple gelator backbone, rationalization of its effect on gelation self-assembly has been critically analyzed with a series of ambidextrous type gelators, N-n-acyl-(L)Val-X-OBn (X = 1,ω-amino acid) by means of various well established physicochemical investigations. Primarily π-π type interaction at the aromatic unit plays a governing role towards the alignment of the gelator molecules. Secondly, positioning of amide unit across the aliphatic chain is found to be crucial for the orientation of peptidic unit in parallel or antiparallel fashion during interdigitated molecular arrangement within the self-assembly. An antiparallel orientation results if the amide unit is deeply seated at a spacer length bigger than the N-acyl unit, however for shorter spacer (i.e., smaller than N-acyl chain) parallel orientation is preferred. Moreover, strength arising from peptidic unit is found to be augmented by the proximal presence of strongly hydrophobic π-π type interactive aromatic units. Increase in methylene units in spacer or in N-acyl unit increases solute-solvent interaction in apolar media however, a polarophobic effect operates in polar media. Manifestation of non-planarity across the amide plane with the increase in gelation concentration as evident from the CD studies strongly suggests an additional conformational

reorientation of the gelator backbone that takes place during the process of self-assembly. Therefore, it is not just the gelator-gelator and gelator-solvent interaction playing their role behind the process of gelation self-assembly, but the conformational reorientation is also taking part during the molecular organization. Considering the effect of solvents on this of self-assembly process, a critical balance of dispersive and directional forces operate in the self-assembly system (including solute and solvent) which can grossly be described as solvophilic/solvophobic interaction of gelators with the solvents. Such interaction is therefore needed to be duly supported by the optimum conformational change at the flexible and/or apparently rigid segments of the gelator backbone for obtaining optimum supramolecular interaction. So far the structure-function relationships are concerned, an increase in N-acyl length, in general, increases the thermal stability whereas the same for spacer region gives reverse results. Molecular packing differs, though not significantly, with the gelator backbone architecture, however, a primitive cubical *Pm3m* type molecular arrangement was unanimously found for either of the xerogels. Significant contribution from intergelator H-bonding interaction was found prevalent in apolar solvents whereas; a polarophobic interaction with a synergic assistance of H-bonding effect becomes predominant in polar media. Solvent-gelator interaction was found to be complex in nature, one solvent parameter system was found insufficient to analyze it, however a dominant influence of δ_h of HSP and α of KT has been observed where both δ_h and α are grossly related to the H-bonding parameter of the solvents of the two different systems. Nevertheless self-assembly is apparently dominated by solvophobic effect. The obtained results significantly demonstrate that non-covalent interaction among the gelator molecules depend on their supramolecular functionalities encrypted in their backbone architecture, but these non-covalent interactions between the molecular backbones and the solvents of gelation should be such that mutually they can overcome the solvation energy but can stabilize self-assembled gel-network with optimum gelator backbone conformation for achieving required enthalpic contribution for self-assembly.

REFERENCES

(1) A. Hirst, I. Coates, T. Boucheteau, J. Miravet, B. Escuder, V. Castelletto,I. Hamley andD. Smith, *J. Am. Chem. Soc,* 2008, **130(28)**, 9113-9121.

(2) P.Terech and R.Weiss, *Chem. Rev,*1997, **97(8)**, 3133-3160.

(3) D. Hatchett and M. Josowicz, *Chem. Rev,* 2008, **108(2)**,746-769.

(4) F.Fages, *Angew. Chem. Int. Ed,* 2006, **45(11)**, 1680-1682.

(5) G.John, S. Jadhav, V. Menonand V. John, *Angew. Chem. Int. Ed,* 2012, **51(8)**, 1760-1762.

(6) Y. Ren, W. Kan, V. Thangaduraiand T. Baumgartner, *Angew. Chem. Int. Ed,* 2012, **51(16)**, 3964-3968.

(7) A. Maity, F. Ali, H. Agarwalla,B. Anothumakkoolband A. Das, *Chem. Commun,* 2015, **51**, 2130-2133.

(8) J. van Esch, *Langmuir,*2009, **25(15)**, 8392–8394.

(9) C. Laqadecand D. Smith, *Chem.Commun,* 2012, **48**, 7817-7819.

(10) R. Service, *Science,* 2005, **309(5731)**, 95.

(11) W.Edwards, C. Lagadec, and D.Smith, K. *Soft Matter,*2011, **7(1)**, 110-117.

 (12) J.Bonnet,G. Suissa,M.Raynal and L. Bouteiller, *Soft Matter*, 2015, **11(11),** 2308-2312.

(13) L. Yaqi, M.Corradini ,X.Liu, T.May , F.Borondics, R.Weissand M.Rogers ,*Langmuir*, 2014, **30(47)**,14128–14142.

(14) A.Hirst, B. Escuder, J.Miravetand D.Smith, *Angew. Chem. Int. Ed,* 2008, **47(42)**, 8002-8018.

(15) K. Rajagopal and J. Schneider, *Curr. Opin. Struct. Biol*. 2004, **14(4)**, 480-486.

(16) C. Wanga, Z. Li, X. Wang, W. Wei, S. Chenband Z. Sui, *Coll. Surf. A. Phys. Eng. Aspct.*, 2011, **384(1-3)**, 490-495.

(17)Y. Huanga, J. Gea, Z. Caia, Z. Huaand X. Honga, *Coll. Surf. A. Phys. Eng. Aspct.,* 2012, **414**, 88-97.

(18) F. Schoonbeek, J. van Esch, R. Hulst, R. Kellogg and B. Feringa, *Chem. –Eur. J.,*2000, **6(14)**, 2633-2643.

(19) J.van Esch, S. de Feyter, R. Kellogg, F.de Schryverand B.Feringa, *Chem. –Eur. J.,*1997, **3(8)**, 1238-1243.

(20) M. Barboiu,S. Cerneaux, A .van der Lee and G. Vaughan, *J. Am. Chem. Soc.,*2004, **126(11)**,3545–3550.

(21) J. Miravet and B. Escuder, *Org. let.* 2005, **7(22)**,4791–4794.

(22) H. Sato, E. Noqami, T. Yajima and A. Yamaqishi, *RSC adv*., 2014, **4(4)**, 1659-1665.

(23) G. Gundert, L. Klein,M. Fischer, F. Vögtle, K. Heuzé, J. Pozzo, M. Vallie and F. Fages, *Angew chem Int. ed. Engl,* 2001, **40(17)**,3164-3166.

(24)G. Kuang,Y. Ji, X. Jia,E. Chen,M. Gao, J. Yeh and Y. Wei, *Chem. Mater.,*2009, **21(3)**, 456–462.

(25) M.Suzuki,T. Sato, H.Shira and, K.Hanabusa, *New. J. Chem.,*2006, **30(8)**, 1184-1191.

(26)S. Datta, S. Samanta and S. Bhattacharya*Chem. –Eur. J.,*2013, **19(34)**, 11364–11373.

(27) S. Halda and, S. Maji, *Coll. Surf. A. Phys. Eng. Aspct.,*2013, **430**, 65-75.

(28) A.S. Krishnan, K.E. Roscov and R.J. Spontak, Advanced Nanomaterials*,* Edited by K. Geckeler and H. Nishide, *,Wiley VCH,* 2010, Vol-I, Chapter 26, pp-824.

(29) R. Weiss, *J. Am. Chem. Soc.,*2014, **136(21)**, 7519–7530.

(30) S. Maji and S. Haldar, *Coll. Surf. A. Phys. Eng. Aspct.,*2012, **414**, 422-432.

(31) S. Ahmed, J. Mondal,N. Behera and D.Das, *Langmuir,*2013,**29(46)**, 14274-14283.

(32) F. Menger andK.Caran, *J. Am. Chem. Soc*2000,**122(47)**, 11679-11691.

(33) G. Zhu and J. Dordick, *Chem. Mater ,*2006, **18(25)**, 5988–5995.

(34) J. Wu, T. Yi, Y. Zou, Q. Xia, T. Shu, F. Liu, Y. Yang, F. Li, Z. Chen,Z. Zhou and C. Huang, *J. Mater. Chem.,*2009, **19(23)**, 3971-3978.

(35) S. Bhattacharya and A. Pal, *J. Phys. Chem. B.,*2008, **112 (16***)*, 4918–4927.

(36)S. Iqbal, J. Miravet and B. Escuder, *Eur. J. Org. Chem.,*2008,**(27)**,4580–4590.

(37) N. Zweep,A. Hopkinson,A. Meetsma, W. Browne, B. Feringa and J. van Esch, *Langmuir,*2009, **25(15)**, 8802 – 8809.

(38)D. Rizkov, J. Gun, O. Lev,R. Sicsic and A. Melman, *Langmuir,*2005,**21(26)**, 12130–12138.

(39) J. Makarević, M. Jokić,Z. Raza,Z. Štefanić,B. Kojić-Prodić and M. Žinić, *Chem. -Eur. J.,*2003, **9(22)**, 5567–5580.

(40) P. Devidson, Molecular Gels: Materials with Self-Assembled Fibrillar Networks, Edited by R. Weiss, P. Terech, *Springer*, 2006, Chapter 26, pp-744.

(41) F. Menger and A. Peresypkin, *J. Am. Chem. Soc.,*2003,**125(18)**, 5340–5345.

(42)P. Terech,D. Pasquier, V. Bordas and C. Rossat, Rheological Properties and Structural Correlations in Molecular Organogels. *Langmuir ,*2000, **16(10)**, 4485–4494.

(43) M. Laupheimer, N. Preisig and C. Stubenrauch, *Coll. Surf. A. Phys. Eng. Aspct.,*2015, **469**, 315–325.

(44) M. Rogers, A. Wright and A. Marangoni, *J. Phys. D: Appl. Phys.,*2008, **41(21)**, 215501 (5pp).

(45) C. Toniol and, M. Palumbo, *Biopolymers,*1977, **16(1)**, 219–224.

(46) A. Barth, *Biochim. Biophy. Acta-Bioenergetics*, 2007,**1767(9)**, 1073-1101.

(47) E. Smith and P. Dea, *Biophys. Chem.,*2015, **196**, 86–91.

(48) J. Shah, Sadhale and D. Chilukuri, *Adv. Drug Deliv. Rev.,*2001, **47(2-3)**, 229–250.

(49)L. Bednárová,P. Maloň and P. Bouř, *Chirality,*2007,**19(10)**, 775-786.

(50) J. Esch and F. Schoo, *Langmu*ir,2004,**20(25)**, 10851–10857.

(52) K. Hanabusa, M. Matsumoto, M. Kimura, A. Kakehi and H Shirai, *J. Colloid Interface Sci.,*2000, **224(2)**, 231–244.

(53) A. Hirst, D. Smith, M. Feiters and H. Geurts, *Langmuir,*2004, **20(17)**, 7070–7077;

(54) J. Hardy, A. Hirst and D. Smith, *Soft Matter*, 2012, **8(12)**, 3399-3406.

(55)J. Makarević, M. Jokić,B. Perić,V. Tomišić,B. Kojić-Prodić and M. Žinić, *Chem. Eur. J.,*2001, **7(15),** 3328-3341.

(56) A. Barton, *Chem. Rev.,*1975, **75(6)**, 731–753.

(57)Y. Loo, E. Wu, A. Lakshmanan, A. Mishra and C. Hauser, Self-Assembled Peptide Nanostructures: Advances and applications in nanobiotechnology, Edited by Jaime Castillo-León, Luigi Sasso and Winnie E. Svendsen , CRC Press,*Taylor & Francis Group*, 2012, Chapter 6, pp-165.

(58) A.Doig and D. Williams, *J. Am. Chem. Soc.,*1992,**114(1)**, 338-343.

(59) V. Mallia and R. Weiss, *J. Phys. Org. Chem.*, 2014, **27(4)**, 310-315.

Figure Captions

Fig.1 Molecular architecture of the gelators [Set-I : **4a**-**4e**; Set-II: **4c**, **4f**, **4g**; Set-III: **4d**, **4h**].

Fig.2 Schematic presentation of the gelators' backbone architecture.

Fig.3 FESEM images of organogels (a) **4d**, (b) **4g** and (c) **4h** in acetonitrile at a concentration of 10 mM

(above CGC) [inset represents the photographs of respective organogels in inverted vials].

Fig. 4 Plots of Gelation Number of different gelators with different hydrophobicity (presented by clogP)

Panel-I for Set-I gelators and Panel-II for Set-II gelators in (a) aromatic, (b) apolar (c) aprotic polar and (d)

in protic polar media.

Fig. 5 Plots of T_{gel} of different gelators with different hydrophobicity (presented by clogP) Panel-I for Set-I

gelators and Panel-II for Set-II gelators in (a) aromatic, (b) apolar (c) aprotic polar and (d) in protic polar

media.

Fig. 6 T_{gel} (°C) versus Gelator concentration (in mM) plot of different gelator in acetonitrile.

Fig. 7 Strain amplitude sweep experiments (at 10 rads/sec) of gelators (a) **4a**, (b) **4c**, (c) **4g**, and (d) **4h** in

acetonitrile.

Fig. 8 Plausible molecular self-assembly of **4d** and **4h**.involving only parallel for **4d** and a mixed-parallel-

antiparallel β-sheet type alignment for 4h of peptidic segment in two mutually orthogonal directions.

Fig. 9 XRD profile of xerogels (intensity vs. 2θ) for **4d** in acetonitrile (I), **4g** in acetonitrile (II) and **4g** in Ethanol [inSet represent s respective plots of d^{-1} vs. $\sqrt{(h^2+l^2+k^2)}$]
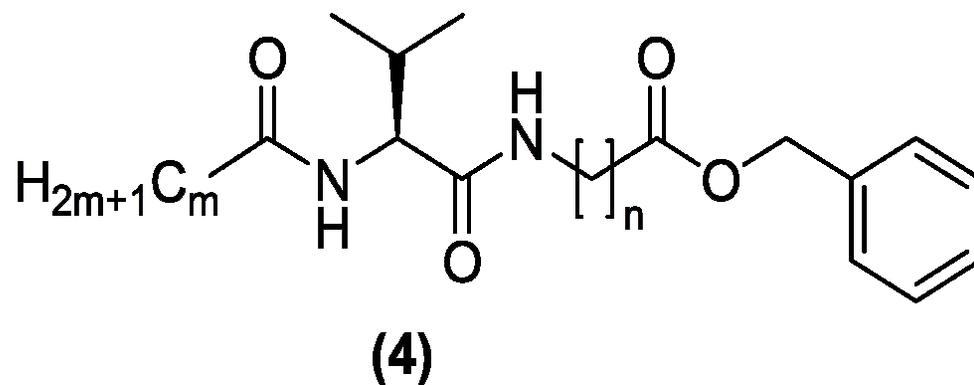
Fig.10 A representative self-assembly of the gelator **4d**. (A) showing the inter layer spacing and (B) interdigitated acyl chains with a parallel β-sheet type arrangement (where spacer length < acyl chain lengh) with a calculated d_{100} value and π-π stacking distance among aromatic groups and (C) interdigitated antiparallel β-sheet type arrangement of **4h** (where spacer length > acyl chain lengh) with calculated d_{100} value.

Fig.11 Concentration dependent CD spectra of **4c**, **4g** and **4d** in CH_3CN.

Fig.12 Plots of, (a)δ_p vs δ_h, (b) δ_d vs δ_h and (c) δ_p vs δ_d (HSP) [panel I] and (a) π* vs. α, (b) β vs. α and (c) βvs. π*(KT) [panel II]of gelators **4a**-**4g** [shaded zones are prevailing area of gelation].

Fig.13 Plausible mechanism behind gelation self-assembly

Fig.1

$H_{2m+1}C_m$ ... (4)

(a) m = 9; n = 2   (d) m = 15; n = 2   (g) m = 13; n = 5
(b) m = 11; n = 2   (e) m = 17; n = 2   (h) m = 7; n = 10
(c) m = 13; n = 2   (f) m = 13; n = 3

1

Fig.2

(i) Aromatic Head (π-π interaction)

(iii)

(ii) Peptidic unit (H-bonding motif)

(iv)

Flexible Hydrophobic spacer (van der Waals interaction)

Structural Modulation (Present work)

Hydrophobic tail (van der Waals interaction)

Fig.3

Fig.4

Fig.5

Fig.6

*T*_{gel} at conc=0.166 mmol

4a=35.23 ⁰C
4b=41.31 ⁰C
4c=48.42 ⁰C
4d=61.23 ⁰C
4e=49.20 ⁰C

*T*_{gel} at conc=0.244 mmol

4a=38.59 ⁰C
4b=50.62 ⁰C
4c=49.60 ⁰C
4d=64.20 ⁰C
4e=52.56 ⁰C

Fig.7

Fig.8

Parallel β-sheet

Parallel β-sheet

4d

Parallel β-sheet

Anti-parallel β-sheet

4h

Fig.9

Fig.10

Fig.11

Fig.12

PANEL - I

PANEL - II

Fig.13